

Adsorption of Formaldehyde on the Ru(001) and Ru(001)-p(2×2)O Surfaces

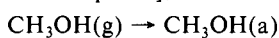
A. B. Anton, J. E. Parmeter, and W. H. Weinberg*

Contribution from the Division of Chemistry and Chemical Engineering, California Institute of Technology, Pasadena, California 91125. Received September 5, 1985

Abstract: The adsorption of formaldehyde on the clean Ru(001) surface and a Ru(001) surface on which an ordered p(2×2) overlayer of oxygen adatoms is present has been investigated via high resolution electron energy loss vibrational spectroscopy and thermal desorption mass spectrometry. On the clean Ru(001) surface, the formaldehyde surface bonding interaction at 80 K is primarily via π_{CO} donation and π_{CO}^* backdonation, leading to decomposition to adsorbed hydrogen and CO for low exposures. With subsequent exposure to formaldehyde, a small fractional surface coverage ($\theta = 0.02\text{--}0.03$) of η^2 -formyl is observed, followed by formation of η^2 -formaldehyde ($\theta = 0.10$) and η^1 -formaldehyde at saturation (monolayer) coverage. Upon heating, the η^2 -formyl decomposes to adsorbed hydrogen and CO by 120 K, and the η^1 -formaldehyde desorbs molecularly between 130 and 180 K. Further heating decomposes the remaining η^2 -formaldehyde, and thermal desorption measurements indicate that a total of a quarter monolayer of formaldehyde decomposes on the Ru(001) surface under these conditions. The presence of the p(2×2)O overlayer ($\theta = 0.25$) withdraws charge from the surface ruthenium atoms, increasing their Lewis acidity and making σ lone pair donation the dominant formaldehyde surface bonding interaction. Under these conditions, only η^1 -formaldehyde is observed for all submonolayer coverages after adsorption at 80 K. After annealing the surface to 300 K to desorb η^1 -formaldehyde, small amounts of η^2 -formaldehyde ($\theta = 0.01$) and η^2 -formate ($\theta = 0.04$) are observed. Compared to the clean surface, more molecular desorption of formaldehyde is observed in the 130–180 K temperature range, and the decomposition activity, as evidenced by the amount of CO and H₂ evolved from the surface, is decreased by a factor of 2 from a quarter to an eighth of a monolayer.

I. Introduction

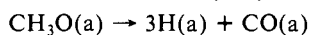
A number of investigations have sought to elucidate the details of the heterogeneously catalyzed reaction of CO with H₂ to form methanol via studies of methanol adsorption and thermal decomposition on single crystalline metal surfaces. Studies on Ni(111),¹ Cu(100),² Pt(111),³ Pd(100),⁴ and Ru(001)⁵ which have included results of electron energy loss spectroscopy (EELS) experiments to identify surface intermediates during the annealing of adsorbed overlayers of methanol have demonstrated the formation of an adsorbed methoxy intermediate [(g) denotes gaseous species and (a) adsorbed species], i.e.,



and



Heating of the surfaces to temperatures near 300 K resulted in decomposition of the adsorbed methoxy to yield H(a) and CO(a):



No stable intermediates other than the methoxy could be isolated, indicating that intermediates in the methoxy decomposition, e.g., H₂CO(a) or HCO(a), are less stable and decompose rapidly compared to the methoxy. The study of the chemisorption and thermal decomposition of formaldehyde on these metal surfaces may afford an opportunity to investigate the structures of adsorbed formaldehyde and formyl intermediates, providing a more complete mechanistic picture of methanol decomposition [and by inference, methanol synthesis from H₂ and CO⁶] in terms of elementary surface reactions. Pursuit of this information provides the motivation for the present study of formaldehyde adsorption on the Ru(001) surface.⁷

An early investigation of formaldehyde adsorption on W(100) and W(111) surfaces employing thermal desorption mass spec-

trometry (TDMS) demonstrated the evolution of H₂ and CO as the principal reaction products, with small amounts of CO₂ and methane produced only at coverages approaching a saturated monolayer.⁸ A more recent TDMS study of formaldehyde adsorption on clean and carbided W(100) surfaces showed qualitatively similar results, but also indicated minority evolution of a small amount of methanol from the clean surface and the evolution of methyl formate together with enhanced formation of methanol and methane from the carbided surface.⁹ On Ni(110), formaldehyde adsorption yielded H₂, CO, CO₂, H₂O, and methanol as reaction products,¹⁰ and a more recent investigation of the same system,¹¹ which also included EELS results to identify surface intermediates, qualitatively duplicated the TDMS results of the previous investigation and showed that, in addition to hydrogen and CO from formaldehyde decomposition, methoxy is the primary surface intermediate, and mixed multilayers of solid formaldehyde and polymeric paraformaldehyde are formed at high coverages. Products similar to those observed for the reaction of formaldehyde with tungsten and nickel surfaces were also reported for clean and sulfided Pt(111) surfaces.¹² On an oxygen precovered Ag(110) surface,¹³ EEL spectra consistent with an η^2 -dioxymethylene species or paraformaldehyde were obtained below 200 K, and decomposition to evolve H₂ and CO₂ through a formate intermediate occurred upon heating the surface to 500 K. Similar results were obtained for formaldehyde adsorption on clean and oxygen precovered Cu(110) surfaces,¹⁴ where EELS identified paraformaldehyde as the only monolayer species on both surfaces at low temperatures. Depolymerization of adsorbed paraformaldehyde released formaldehyde from both surfaces at 225 K. However, EEL spectra for the oxygen precovered surface showed that a reaction of formaldehyde with coadsorbed oxygen also occurred, producing adsorbed formate which decomposed to yield CO₂ and H₂ near 470 K.

More pertinent to the results reported here are studies of the homogeneous chemistry and structures of coordinated formaldehyde and formyl.¹⁵⁻¹⁷ Several stable compounds displaying

(1) Demuth, J. E.; Ibach, H. *Chem. Phys. Lett.* **1979**, *60*, 395.

(2) Sexton, B. A. *Surf. Sci.* **1979**, *88*, 299.

(3) Sexton, B. A., *Surf. Sci.* **1981**, *102*, 271.

(4) Christmann, K.; Demuth, J. *J. Chem. Phys.* **1982**, *76*, 6308.

(5) Hrbek, J.; de Paola, R. A.; Hoffmann, F. M. *J. Chem. Phys.* **1984**, *81*, 2818.

(6) Henrici-Olivé, G.; Olivé, S. *Agnew. Chem., Int. Ed. Engl.* **1976**, *15*, 136.

(7) Anton, A. B.; Parmeter, J. E.; Weinberg, W. H. *J. Am. Chem. Soc.* **1985**, *107*, 5558.

(8) Yates, J. T.; Madey, T. E.; Dresser, M. J. *J. Catal.* **1973**, *30*, 260.

(9) Benziger, J. B.; Ko, E. I.; Madix, R. J. *J. Catal.* **1980**, *64*, 132.

(10) Dickinson, J. T.; Madix, R. J. *Int. J. Chem. Kinet.* **1978**, *10*, 871.

(11) Richter, L. J.; Ho, W. *J. Chem. Phys.* **1985**, *83*, 2165.

(12) Abbas, N. M.; Madix, R. J. *Appl. Surf. Sci.* **1981**, *7*, 241.

(13) Stuve, E. M.; Madix, R. J.; Sexton, B. A. *Surf. Sci.* **1982**, *119*, 279.

(14) Sexton, B. A.; Hughes, A. E.; Avery, N. R. *Surf. Sci.* **1985**, *155*, 366.

$\eta^2(\text{O,C})$ coordination geometries [bonded to the metal atom(s) through both the oxygen and carbon atoms of the carbonyl, hereafter referred to simply as η^2] for formaldehyde¹⁸⁻²¹ and acetaldehyde²² have been synthesized and characterized structurally. Furthermore, evidence for $\eta^1(\text{O})$ coordination [bonded end-on to the metal atom through only the oxygen atom, hereafter referred to simply as η^1] has been obtained for a formaldehyde complex of ruthenium.²³ Structures analogous to both of these have been observed for the adsorption of the structurally similar acetone molecule on the Ru(001) surface.²⁴ Finally, η^1 -formyl,^{23,25-29} η^2 -formyl,³⁰⁻³² and similar η^1 -acyl complexes³³⁻³⁷ have also been synthesized and characterized structurally.

This paper presents an EELS and TDMS investigation of the adsorption and reactions of formaldehyde on both the clean Ru(001) surface and a Ru(001) surface modified chemically by the presence of an ordered p(2×2) overlayer of oxygen adatoms. The results of the experiments conducted on the clean Ru(001) surface differ from those described earlier for other single crystalline metal surfaces in that no evidence for associative reactions on the surface is obtained. Instead, only reversible molecular adsorption and decomposition to hydrogen and CO through intermediates similar to those observed in the homogeneous chemistry of model CO hydrogenation reactions are observed. Addition of the p(2×2) oxygen overlayer not only provides an adsorbed reactant which may open surface reaction channels that did not exist on the clean surface, but it also withdraws charge from the surface ruthenium atoms, increasing their Lewis acidity and altering their reactivity toward the reactions identified on the clean surface. The results obtained for formaldehyde adsorption and decomposition provide an interesting and chemically consistent comparison to those obtained previously for the adsorption of acetone on the same clean and oxygen modified surfaces.²⁴

II. Experimental Procedures

A description of the EEL spectrometer and the UHV system in which it is contained has been published previously.³⁸ EEL spectra were

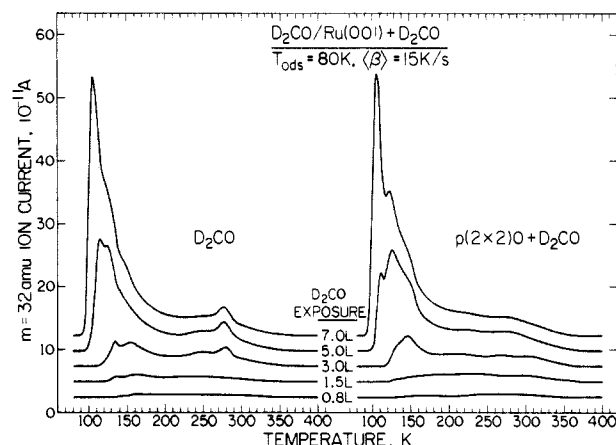


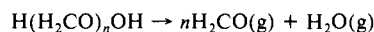
Figure 1. Thermal desorption spectra for increasing exposures of D_2CO on the clean Ru(001) (left) and Ru(001)-p(2×2)O (right) surfaces at 80 K. The average heating rate, $\langle\beta\rangle$, for these spectra and the spectra of Figures 2 and 3 was 15 K/s.

recorded at a resolution of 80 cm^{-1} (full-width at half-maximum) with a count rate of $3 \times 10^5\text{ Hz}$ in the specularly reflected, elastically scattered electron beam. Incident electron beam kinetic energies at the sample were 5–6 eV.

The Ru(001) surface was cleaned by using standard techniques of Ar^+ sputtering and annealing in oxygen.³⁹ Surface cleanliness was monitored via both EELS and TDMS. The ordered p(2×2) overlayer of oxygen adatoms, with an ideal surface coverage of 0.25 monolayer, was prepared by exposing the clean surface to 0.8 L of O_2 ($1\text{ L} \equiv 10^{-6}\text{ torr}\cdot\text{s}$) at 95 K, followed by thermal ordering at a temperature of approximately 350 K.^{40,41}

Gaseous H_2CO and D_2CO were produced by thermal dehydration and depolymerization of their parent polyoxymethylene glycols (paraformaldehyde), and the crystal surface was exposed to these gases by back-filling the UHV chamber through leak valves. Exposures quoted in the text were measured with a Bayard-Alpert ionization gauge, uncorrected for relative ionization cross sections.

The formaldehyde used in these experiments was purified by extensive pumping on the solid paraformaldehyde prior to thermal depolymerization. Storage lines which held formaldehyde prior to introduction into the UHV chamber were cleaned and refilled frequently, and the composition of the vapor introduced into the UHV chamber was checked in situ via mass spectrometry. Water is an unavoidable product of the thermal depolymerization reaction⁴²



and high grade paraformaldehydes as were used in this work [H_2CO from Aldrich Chemical Co., and D_2CO from U.S. Services Inc. (98 atom % D)] have an average degree of polymerization near 30. Thus the vapor produced by thermal depolymerization is expected to contain approximately 3 mol % water. Further purification of the vapor, for example, by treatment with standard chemical drying agents, is in general fruitless, since these materials also catalyze the decomposition and polymerization of formaldehyde.⁴² Fortunately, the adsorption properties of water on both the clean⁴³ and oxygen precovered⁴⁴ Ru(001) surfaces have been characterized thoroughly by both TDMS and EELS, allowing extraction from the EEL spectra for formaldehyde adsorption those features attributable to the presence of small amounts of coadsorbed water after annealing of the surface to temperatures below 170 K, the low coverage desorption temperature for water on Ru(001). Another impurity in formaldehyde that is produced from depolymerization of paraformaldehyde is methyl formate.^{8,42}

Although the formaldehyde used previously⁸⁻¹⁴ was prepared by methods nearly identical with those employed here, in most cases little or no mention is made of the presence of water and methyl formate

- (15) Muetterties, E. L.; Stein, J. L. *Chem. Rev.* **1979**, *79*, 479.
 (16) Masters, C. *Adv. Organomet. Chem.* **1979**, *17*, 61.
 (17) Dombek, B. D. *J. Am. Chem. Soc.* **1980**, *102*, 6855.
 (18) Brown, K. L.; Clark, G. R.; Headford, C. E. L.; Marsden, K.; Roper, W. R. *J. Am. Chem. Soc.* **1979**, *101*, 503.
 (19) Gambarotta, S.; Floriani, C.; Chiesi-Villa, A.; Gaustini, C. *J. Am. Chem. Soc.* **1982**, *104*, 2019; **1985**, *107*, 2985.
 (20) Buhro, W. E.; Patton, A. T.; Strouse, C. E.; Gladysz, J. A. *J. Am. Chem. Soc.* **1983**, *105*, 1056.
 (21) Kropp, K.; Skibbe, Y.; Erker, G.; Krüer, K. *J. Am. Chem. Soc.* **1983**, *105*, 3353.
 (22) Adams, H.; Bailey, N. A.; Gauntlett, J. T.; Winter, M. J. *J. Chem. Soc., Chem. Commun.* **1984**, 1360.
 (23) Chaudret, B. N.; Cole-Hamilton, D. J.; Nohr, R. S.; Wilkinson, G. *J. Chem. Soc., Dalton Trans.* **1977**, 1546.
 (24) Avery, N. R.; Weinberg, W. H.; Anton, A. B.; Toby, B. H. *Phys. Rev. Lett.* **1983**, *51*, 682. Anton, A. B.; Avery, N. R.; Toby, B. H.; Weinberg, W. H. *J. Am. Chem. Soc.*, in press.
 (25) Thorn, D. L. *J. Am. Chem. Soc.* **1980**, *102*, 7109; *Organomet.* **1982**, *1*, 197.
 (26) Wong, W.-K.; Tam, W.; Strouse, C. E.; Gladysz, J. A. *J. Chem. Soc., Chem. Commun.* **1979**, 530.
 (27) Casey, C. P.; Neumann, S. M.; Andrews, M. A.; McAlister, D. P. *Pure Appl. Chem.* **1980**, *52*, 625.
 (28) Morton, J. R.; Preston, K. F. *Chem. Phys. Lett.* **1984**, *111*, 611.
 (29) Casey, C. P.; Meszaros, M. W.; Neumann, S. M.; Cesas, I. G.; Haller, K. *J. Organomet.* **1985**, *4*, 143.
 (30) Moloy, K. G.; Marks, T. J. *J. Am. Chem. Soc.* **1984**, *106*, 7051.
 Marks, T. J. *Science (Washington, D.C.)* **1982**, *217*, 989.
 (31) Belmonte, P. A.; Clarke, F. G. N.; Schrock, R. R. *J. Am. Chem. Soc.* **1983**, *105*, 2643. Churchill, M. R.; Wasserman, H. J. *Inorg. Chem.* **1983**, *21*, 226.
 (32) Wolczanski, P. T.; Bercaw, J. E. *Acc. Chem. Res.* **1980**, *13*, 121.
 (33) Roper, W. R.; Taylor, G. E.; Waters, J. M.; Wright, L. J. *J. Organomet. Chem.* **1979**, *182*, C46.
 (34) Sükél, K.; Schlöter, K.; Beck, W.; Ackerman, K.; Schubert, U. J. *Organomet. Chem.* **1983**, *241*, 333.
 (35) Merlino, S.; Montagnoli, G.; Braca, G.; Sbrana, G. *Inorg. Chim. Acta* **1978**, *27*, 233.
 (36) Longato, B.; Norton, J. R.; Huffmann, J. C.; Marsella, J. A.; Caulton, K. G. *J. Am. Chem. Soc.* **1981**, *103*, 209.
 (37) Bristow, G. S.; Hitchcock, P. B.; Lappert, M. F. *J. Chem. Soc., Chem. Commun.* **1982**, 462.

- (38) Thomas, G. E.; Weinberg, W. H. *Rev. Sci. Instrum.* **1979**, *50*, 497.
 (39) Thomas, G. E.; Weinberg, W. H. *J. Chem. Phys.* **1979**, *70*, 954.
 (40) Rahman, T. S.; Anton, A. B.; Avery, N. R.; Weinberg, W. H. *Phys. Rev. Lett.* **1983**, *51*, 1979.
 (41) Madey, T. E.; Engelhardt, H. A.; Menzel, D. *Surf. Sci.* **1975**, *48*, 304.
 (42) Walker, J. F. "Formaldehyde", 3rd ed.; Reinhold: New York, 1964; pp 44–45, 215.
 (43) Thiel, P. A.; Hoffmann, F. M.; Weinberg, W. H. *J. Chem. Phys.* **1981**, *75*, 5556.
 (44) Thiel, P. A.; Hoffmann, F. M.; Weinberg, W. H. *Phys. Rev. Lett.* **1982**, *49*, 501.

impurities and their potential importance on the chemistry of the surfaces investigated. For example, small amounts of methane, carbon dioxide, and methyl formate evolution in TDMS after large formaldehyde exposures.^{8,9,12} may be due to the adsorption and/or reaction of a methyl formate contaminant. Furthermore, the polymerization of formaldehyde to give adsorbed paraformaldehyde^{11,13,14} may not result from the interaction of formaldehyde with the clean metal surface but rather from the interaction of formaldehyde with adsorbed water, which is known to catalyze formaldehyde polymerization rapidly on rather nonreactive surfaces below 100 °C.⁴²

Thermal desorption measurements were made in a line-of-sight configuration with a UTI 100C quadrupole mass spectrometer, oriented approximately 40° from the surface normal. Surface coverages of H₂ and CO reported for the reaction product TDMS measurements were obtained by comparing the time integrated ion current of the desorption spectra to those obtained for desorption of known coverages of H₂⁴⁵ and CO⁴⁶ and are accurate to approximately 10%.

III. Results

A. Thermal Desorption Spectra of Formaldehyde from the Clean Ru(001) and the Ru(001)-p(2×2)O Surfaces. Thermal desorption spectra of D₂CO recorded after the indicated exposures of the clean Ru(001) surface and the Ru(001)-p(2×2)O surface to D₂CO at 80 K are shown at the left and right of Figure 1, respectively. For exposures of 0.8 L or less of D₂CO on both surfaces, no molecular formaldehyde desorption is observed. For exposure of the clean surface to 1.5 L or more of D₂CO, desorption rate maxima associated with monolayer adsorbed states appear near 130 and 155 K. These peaks saturate and shift slightly to lower temperatures for exposures of 5 L or more. Another peak appears near 110 K, the amplitude of which grows without saturation for increasing exposures, indicating that it is associated with multilayers of formaldehyde condensed on the surface. A small sharp peak is also evident near 275 K for exposures of 3 L or more. Activation energies for desorption for the monolayer states desorbing at 130, 155, and 275 K, estimated for first-order desorption kinetics via the method of Redhead with $\nu = 10^{13} \text{ s}^{-1}$,⁴⁷ are 7.3, 8.8, and 16.0 kcal/mol, respectively. Similar results are obtained for desorption from the Ru(001)-p(2×2)O surface, although desorption from the monolayer states near 130 and 155 K is enhanced for equivalent exposures compared to the clean surface, and the state at 275 K is extinguished.

B. Thermal Desorption Spectra of the Decomposition Products, CO and H₂, from Formaldehyde on the Clean Ru(001) and the Ru(001)-p(2×2)O Surfaces. To check for the possible formation of surface reaction products like those identified in earlier studies of formaldehyde adsorption, thermal desorption spectra were recorded at $m = 20$ amu (D₂O⁺, CD₄⁺), $m = 34$ amu (CD₃O⁺ the principal cracking fragment of CD₃OD), $m = 44$ amu (CO₂⁺), and $m = 64$ amu (DCOOC₃⁺), in addition to $m = 4$ amu and $m = 28$ amu for the principal reaction products, D₂ and CO. No desorption at $m = 44$ and $m = 64$ amu was detected for monolayer saturation exposures of both the clean Ru(001) and the Ru(001)-p(2×2)O surfaces to D₂CO at 80 K, and only weak features with intensities lower than those observed for D₂ and CO by factors of 100–1000 were observed at 160–180 K for D₂O and 280–320 K for CD₃OD. Consequently, all D₂O and CD₃OD evolved from both the clean Ru(001) and the Ru(001)-p(2×2)O surfaces are due to impurities in the adsorbed D₂CO. The only desorption products resulting from the interaction of D₂CO with both surfaces are D₂CO, D₂, and CO. Noteworthy in these results is the absence of significant D₂O production from the reaction of deuterium adatoms from D₂CO decomposition with the oxygen adatoms of the p(2×2)O overlayer. This is because the p(2×2)O overlayer destabilizes adsorbed hydrogen into a new binding state with a reduced activation energy for desorption, to be discussed below, decreasing the barrier to hydrogen adatom recombination and desorption.

Thermal desorption spectra of CO recorded after exposure at 80 K of both the clean Ru(001) and the Ru(001)-p(2×2)O

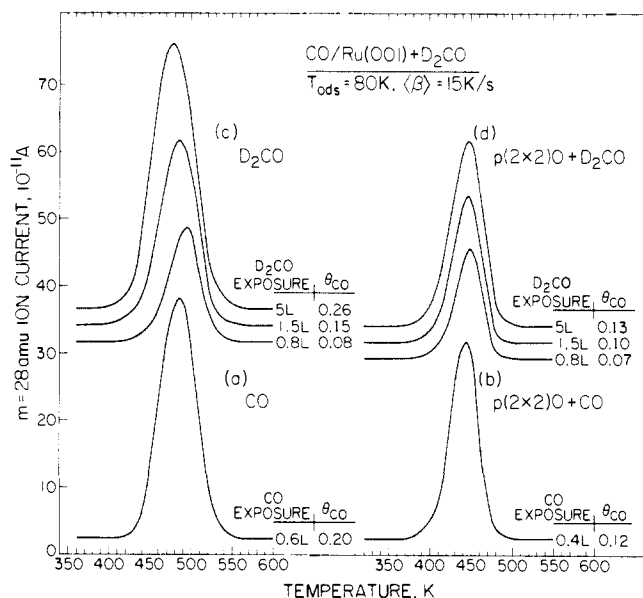


Figure 2. Thermal desorption spectra showing the evolution of CO from Ru(001) following exposure (a) of the clean surface to 0.5 L of CO, (b) of the Ru(001)-p(2×2)O surface to 0.4 L of CO, and (c) of the clean and (d) the Ru(001)-p(2×2)O surfaces to the indicated exposures of D₂CO.

surfaces to 0.8, 1.5, and 5.0 L (monolayer saturation) of D₂CO are shown at the top of Figure 2. Also shown for comparison at the bottom of Figure 2 are spectra recorded after the adsorption of CO. In all these spectra, fractional surface coverages are assigned by comparison to spectra recorded for saturation exposures of the clean surface to CO, where θ_{CO} = adsorbed CO molecules per ruthenium surface atom = 49/75 at saturation.⁴⁶ Since no other reaction products were observed, the CO coverages indicate directly the amount of D₂CO decomposition. For 0.8 L exposures of both surfaces to D₂CO, comparable amounts of decomposition are observed, 0.08 monolayer on the clean Ru(001) surface and 0.07 monolayer on the Ru(001)-p(2×2)O surface. As the D₂CO exposure is increased, however, decomposition on the clean surface increases relative to that on the oxygen pre-covered surface, and for 5-L (monolayer saturation) exposures on both surfaces, the decomposition activity of the clean surface [$\theta_{CO} = 0.26$] is twice that of the Ru(001)-p(2×2)O surface [$\theta_{CO} = 0.13$]. The peak shapes and positions are unperturbed compared to those resulting from adsorption of CO on the same surfaces, suggesting that the surfaces are free of other adsorbed species which could affect the CO desorption rate.

Thermal desorption spectra of D₂ from the decomposition of adsorbed D₂CO, following exposures of both surfaces to D₂CO equal to those used to generate the CO thermal desorption spectra of Figure 2, are shown at the top of Figure 3. For comparison, thermal desorption spectra after D₂ adsorption on both surfaces are shown at the bottom of Figure 3. Coverages for all the spectra are assigned by comparison to the 4.0-L (monolayer saturation) exposure of D₂ on the clean surface where $\theta_D = 0.85$.⁴⁵

Of particular interest are the spectra recorded for the adsorption of D₂ on the Ru(001)-p(2×2)O surface, shown at the bottom of Figure 3. Comparison to the 0.2-L spectrum for D₂ adsorption on the clean surface immediately above shows that the average probability of adsorption up to a coverage of approximately $\theta_D = 0.15$ is increased by a factor of two on the Ru(001)-p(2×2)O surface relative to the clean surface. Desorption of D₂ is complete by 250 K, indicating that the activation energy for desorption is less than 9 kcal/mol [estimated for second-order desorption kinetics via the method of Redhead with $\nu = 10^{-4} \text{ cm}^2 \text{ s}^{-1}$,⁴⁷], as compared to 17.0 kcal/mol on the clean surface.⁴⁵ The peak near 200 K shifts downward with increasing coverage, indicative of second-order desorption kinetics, and at saturation this state contains 0.23 monolayer of deuterium adatoms. The state at lower temperature, which fills after the state at 200 K and is shown

(45) Shimizu, H.; Christmann, K.; Ertl, G. *J. Catal.* **1980**, *61*, 412.

(46) Williams, E. D.; Weinberg, W. H. *Surf. Sci.* **1979**, *82*, 93.

(47) Redhead, P. A. *Vacuum* **1962**, *12*, 203.

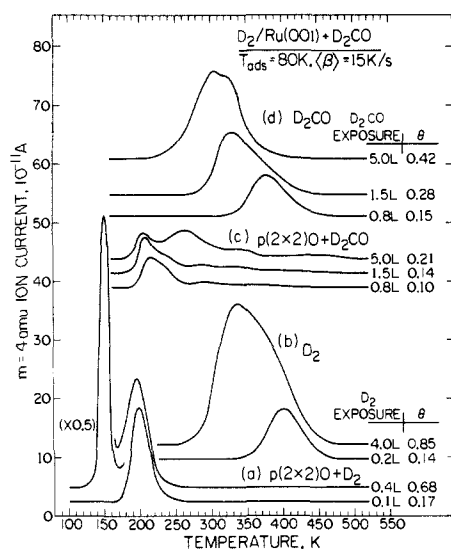
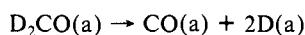


Figure 3. Thermal desorption spectra showing the evolution of D_2 from Ru(001) following the indicated exposures of (a) the Ru(001)- $p(2 \times 2)O$ and (b) the clean Ru(001) surfaces to D_2CO .

expanded by a factor of 0.5 in Figure 3, contains an additional 0.45 monolayer of deuterium adatoms, and its peak temperature remains constant at 150 K from its initial appearance to the exposure necessary for its saturation (0.4 L). The 2:1 stoichiometry of these two states, plus the near match of their populations to the 0.25 monolayer ideal coverage of the $p(2 \times 2)O$ overlayer, suggests that occupation of the state at 200 K contributes stoichiometrically one deuterium atom per $p(2 \times 2)O$ unit cell, and occupation of the state at 150 K contributes an additional two deuterium atoms per $p(2 \times 2)O$ unit cell. Other experiments⁴⁸ have shown that the appearance of both these states is intimately related to the presence of the $p(2 \times 2)O$ overlayer. As the ordered oxygen coverage is increased past 0.25 monolayer, the resulting overlayer is a combination of local regions of both the $p(2 \times 2)$ and the $p(1 \times 2)$ overlayer,⁴⁰ which is developed fully at an oxygen coverage of 0.50 monolayer and does not chemisorb hydrogen at these temperatures. For ordered oxygen adatom coverages below 0.25 monolayer, the thermal desorption spectra of adsorbed D_2 are a linear combination of the clean surface and the surface on which the $p(2 \times 2)O$ overlayer is present.

The stoichiometry of the overall decomposition reaction for formaldehyde



indicates that, in the absence of other surface reactions which consume deuterium, the coverages obtained for the thermal desorption spectra of D_2 at the top of Figure 3 should be twice the coverages obtained for the CO TDMS data of Figure 2. Agreement is obtained within experimental error.

For the thermal desorption spectra obtained after adsorption of D_2CO on the clean Ru(001) surface, all D_2 evolution can be attributed to desorption from the surface after D_2CO decomposition at lower temperature, since the peak shapes and positions match very closely those obtained for the coadsorption of H_2 and CO on Ru(001).⁴⁹ On the Ru(001)- $p(2 \times 2)O$ surface, however, features at temperatures above approximately 250 K are clearly due to the decomposition of adsorbed species in this temperature range, as can be deduced by comparison to the spectra for the Ru(001)- $p(2 \times 2)O$ surface shown in Figure 3a and c.

The decreased decomposition activity of the Ru(001)- $p(2 \times 2)O$ surface compared to the clean Ru(001) surface could be attributed reasonably to a decreased amount of formaldehyde adsorption into monolayer states on the oxygen precovered surface, resulting from blocking by the oxygen adatoms of the $p(2 \times 2)$ overlayer of

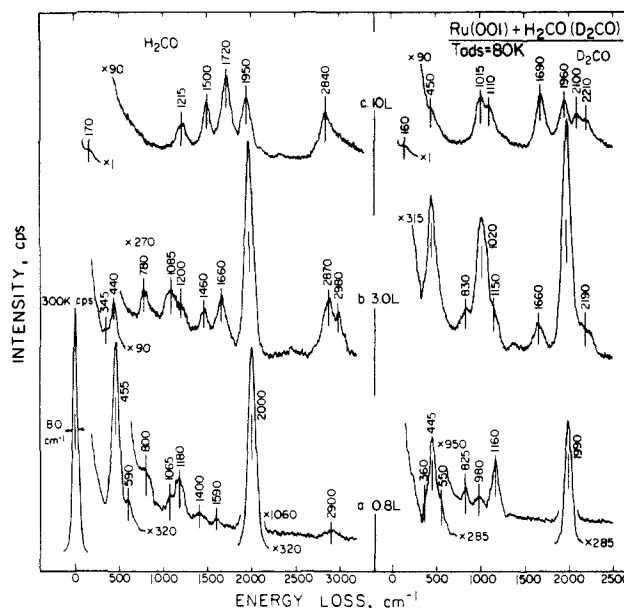


Figure 4. EEL spectra recorded after the indicated exposures of the clean Ru(001) surface to H_2CO (left) and D_2CO (right) at 80 K.

formaldehyde adsorption sites which would otherwise be available on the clean surface. Since the temperature of formaldehyde adsorption, 80 K, is well below the temperature of desorption of condensed multilayers of formaldehyde, 110 K, formaldehyde molecules striking either the clean or the Ru(001)- $p(2 \times 2)O$ surface during exposure at 80 K are expected to adsorb with a probability near unity. Then, the exposures necessary to initiate formation of the multilayer state on each surface in the thermal desorption spectra for formaldehyde give a relative measure of how much formaldehyde is adsorbed into the monolayer states on both surfaces. As may be seen in Figure 1, no desorption from the multilayer state is observed for 3-L exposures of both the clean Ru(001) and the Ru(001)- $p(2 \times 2)O$ surfaces to D_2CO , whereas 5-L exposures produce multilayer desorption from both surfaces. The multilayer state shows greater population for a 5-L exposure of the clean Ru(001) surface to formaldehyde than the Ru(001)- $p(2 \times 2)O$ surface, indicating that more adsorption into monolayer states occurs on the oxygen precovered surface than on the clean Ru(001) surface. Thus, the decreased decomposition activity of the Ru(001)- $p(2 \times 2)O$ surface, compared to the clean Ru(001) surface, must be due to the differences in the reactivity of the adsorbed formaldehyde present on the two surfaces and is not due simply to differences in the amounts of formaldehyde adsorbed.

C. EELS of Formaldehyde on the Clean Ru(001) Surface. EEL spectra recorded after increasing exposures of the clean Ru(001) surface to both H_2CO and D_2CO are shown in Figure 4. For exposures below approximately 0.5 L, total decomposition at 80 K is evidenced by the appearance of only strong vibrational features near 450 and 2000 cm^{-1} due to approximately 0.10 monolayer of adsorbed CO.³⁹ Features attributable to hydrogen or deuterium adatoms from formaldehyde decomposition are not detected due to their extremely small inelastic scattering cross section on the Ru(001) surface.⁵⁰ After a 0.8-L exposure, however, the EEL spectrum of H_2CO shows modes due to other surface species at 590, 800, 1065, 1180, 1400, 1590, and 2900 cm^{-1} . Heating the surface to 120 K causes the modes at 590, 1065, 1180, 1400, and 2900 cm^{-1} to disappear, leaving features at 800 and 1590 cm^{-1} and increasing the intensities of the features due to adsorbed CO by an amount consistent with an increase of the CO coverage of 0.02–0.03 monolayer. Similar results are observed for identical experiments for the adsorption of D_2CO : heating the surface to 120 K removes features near 550 (shoulder), 825,

(48) Anton, A. B.; Weinberg, W. H.; unpublished results.

(49) Peebles, D. E.; Schreifels, J. A.; White, J. M. *Surf. Sci.* **1982**, *116*, 117.

(50) Barteau, M. A.; Broughton, J. Q.; Menzel, D. *Surf. Sci.* **1983**, *133*, 443.

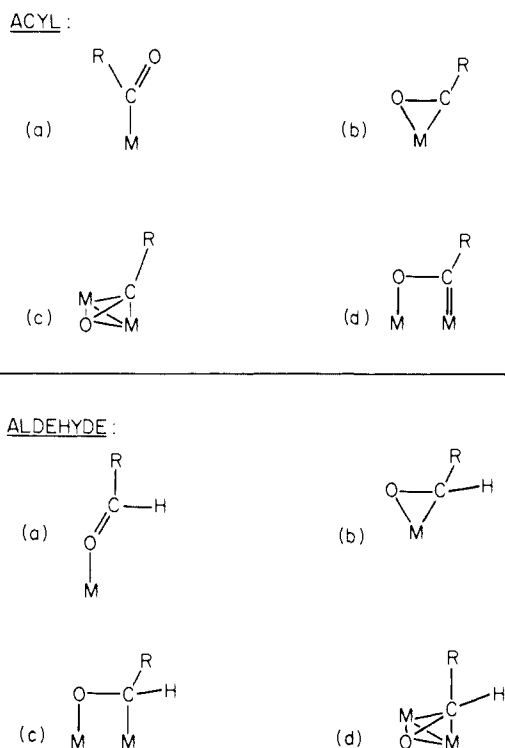


Figure 5. Schematic η^1 [(a) and η^2 [(b), (c), and (d)] bonding configurations observed in homogeneous complexes with acyl (top) and aldehyde (bottom) ligands.

980, and 1160 cm^{-1} , leaving the shoulder near 360 cm^{-1} and a weak feature at 1150 cm^{-1} . A feature for D_2CO corresponding to that at 2900 cm^{-1} for H_2CO should appear near 2100 cm^{-1} , but would be expected to be quite weak and is not resolved from the tail of the strong feature due to $\nu(\text{CO})$ at 1990 cm^{-1} . Spectra which were extended to higher loss energies also showed very weak features at 3500 cm^{-1} for H_2CO and 2500 cm^{-1} for D_2CO which were present both before and after annealing to 120 K. By comparison to EEL spectra obtained for water adsorption on Ru(001),⁴³ the modes at 800 (360), 1590 (1150), and 3500 (2500) cm^{-1} can be readily assigned to librational modes (frustrated translation), $\delta(\text{H}_2\text{O})$ [$\delta(\text{D}_2\text{O})$] and $\nu(\text{OH})$ [$\nu(\text{OD})$], respectively, of less than 0.01 monolayer of adsorbed H_2O (D_2O) from paraformaldehyde depolymerization. The other features are due to a weakly stable species which is an intermediate in the formaldehyde decomposition to hydrogen adatoms and adsorbed CO.

Due to the prevalence of the formyl ligand in organometallic chemistry, such a species must be considered as a possible intermediate in the decomposition of formaldehyde on the Ru(001) surface. Indeed, the vibrational spectra shown in Figure 4a are consistent with a formyl intermediate bound to the surface in an η^2 configuration (see also Figure 5). A comparison of the spectra in Figure 4a for H_2CO and D_2CO allows immediate identification of the modes at 1180 and 1160 cm^{-1} as being due to the carbon-oxygen stretching vibration. The low frequency indicates that the carbon-oxygen bond order is lowered to nearly one, signifying η^2 coordination to the surface. With this established, the remaining modes for η^2 -HCO can be assigned as follows: $\delta(\text{HCO})$, the in-plane deformation at 1400 cm^{-1} ; $\pi(\text{CH})$, the out-of-plane deformation at 1065 cm^{-1} ; and $\nu(\text{CH})$, at 2900 cm^{-1} . The corresponding modes for η^2 -DCO are at 980, 825, and near 2100 cm^{-1} (not resolved). Substantial justification for these assignments and the postulated η^2 coordination geometry for formyl on Ru(001) can be obtained by comparison to the normal mode frequencies for the model compounds HCOOCH_3 and DCOOCH_3 ,⁵¹ where the HCO and DCO functions of each compound mimic in carbon-oxygen bond order and structural arrangement

Table I. Assignments of Vibrational Bands (in cm^{-1}) Observed with High Resolution Electron Energy Loss Spectroscopy of η^2 -HCO and η^2 -DCO on Ru(001)^a

mode	η^2 -HCO	HCOOCH_3 ⁵¹	η^2 -DCO	DCOOCH_3 ⁵¹
$\nu(\text{CH})$	2900	2943		2216
$\delta(\text{CH})$	1400	1371	980	1048
$\nu(\text{CO})$	1180	1207	1160	1213
$\pi(\text{CH})$	1065	1032	825	870
$\nu(\text{Ru-HCO})$	590		550	

^a Also listed for comparison are the IR bands for the HCO and DCO functions of the model compounds HCOOCH_3 and DCOOCH_3 .

the geometry expected for η^2 -formyl on the Ru(001) surface. As may be seen from the results listed in Table I, the correspondence is excellent. The mode at 590 cm^{-1} for η^2 -HCO, appearing as a shoulder near 550 cm^{-1} for η^2 -DCO, is assigned as the frustrated translation of the formyl perpendicular to the surface.

Exposure of the clean Ru(001) surface to 3.0 L of H_2CO or D_2CO [cf. Figure 4b] adds new features to the EEL spectra which signify the presence of surface species other than η^2 -formyl. The appearance of a carbonyl band at 1660 cm^{-1} in both spectra, by analogy to the results obtained for adsorption of the structurally similar acetone molecule on Ru(001),²⁴ indicates the presence of molecular formaldehyde coordinated to the surface in an η^1 configuration. This bonding configuration, shown schematically in (a) in the bottom panel of Figure 5, results from overlap of a single lobe of the nonbonding lone pair orbital of formaldehyde, localized strongly on the oxygen atom, with a d_s hybrid acceptor orbital of the metal, resulting in a net transfer of electron density from the formaldehyde ligand to the metal surface. This σ -donation interaction leaves the skeleton of the formaldehyde molecule unperturbed other than the red-shift of $\nu(\text{CO})$ to 1660 cm^{-1} from its value of 1744 cm^{-1} for free H_2CO and 1700 cm^{-1} for free D_2CO .⁵² Since the remaining features in both spectra cannot all be attributed to η^1 -formaldehyde, another surface species is also present under these conditions. The features at 345 and 780 cm^{-1} in the spectrum for H_2CO are due to the frustrated translational and librational modes of coadsorbed H_2O , respectively,⁴³ and the corresponding modes in the spectrum of D_2CO are not resolved from the tail of the elastic peak and the strong feature due to adsorbed CO near 450 cm^{-1} . Having identified η^1 -formaldehyde by the presence of $\nu(\text{CO})$ at 1660 cm^{-1} , the assignments of the remaining features in these spectra and the structural identification of other species present is best left for the discussion of subsequent spectra, where each species is isolated and characterized unambiguously.

The addition of another 7 L of formaldehyde to the clean Ru(001) surface to give a total exposure of 10 L at 80 K produces condensed multilayers of formaldehyde, as was shown in the TDMS results of Figure 1. EEL spectra recorded for H_2CO and D_2CO under these conditions are shown in Figure 4c, and assignments and corresponding frequencies for solid H_2CO and D_2CO ⁵³ are listed in Table II. As was observed for multilayer adsorption of formaldehyde on Ag(110),¹³ a strong lattice vibration appears at 170 cm^{-1} for H_2CO (160 cm^{-1} for D_2CO), and the frequencies for all other vibrations correspond more closely to those of solid formaldehyde⁵³ than to those of gaseous formaldehyde.⁵² The intensity of $\nu(\text{CO})$ due to adsorbed CO in these spectra indicates that decomposition of approximately 0.15 monolayer of formaldehyde occurs upon adsorption at 80 K.

Shown in Figure 6 are EEL spectra recorded after exposure of the clean Ru(001) surface to 10 L of H_2CO (left) and 10 L of D_2CO (right), followed by annealing to the indicated temperatures. After annealing to 150 K, the mode at 1660 cm^{-1} evident in the 3.0-L spectra of Figure 4b for both H_2CO and D_2CO is absent, indicating that η^1 -formaldehyde has desorbed by this temperature and correlating well with the evolution of form-

(51) Shimanouchi, T. "Tables of Vibrational Frequencies"; Consolidated Vol. 1, NSRDS-NBS 39; Vol. II.

(52) Herzberg, G. "Infrared and Raman Spectra of Polyatomic Molecules"; Van Nostrand: New York, 1945.

(53) Khoshkoo, H.; Hemple, S. T.; Nixon, E. R. *Spectrochim. Acta, Part A* 1974, 30A, 863.

Table II. Assignments of Vibrational Bands (in cm^{-1}) Observed with High Resolution Electron Energy Loss Spectroscopy of H_2CO and D_2CO on Ru(001) and Ru(001)-p(2 \times 2)O^a

mode and sym. for free formaldehyde	Ru(001) and Ru(001)-p(2 \times 2)O							
	solid ⁵³		H_2CO			D_2CO		
	H_2CO	D_2CO	multilayer	$\eta^1(80\text{ K})$	$\eta^2(250\text{ K})$	multilayer	$\eta^1(80\text{ K})$	$\eta^2(250\text{ K})$
$\nu_a(\text{CH}_2)(\text{B}_1)$	2843	2214	2840	2970	2940	2210	2200–2250	2225
$\nu_s(\text{CH}_2)(\text{A}_1)$	2831	2095		2850		2100		
$\nu(\text{CO})(\text{A}_1)$	1700	1660	1720	1660–1680	980	1690	1640–1660	1020
$\delta(\text{CH}_2)(\text{A}_1)$	1490	1096	1500	1465	1450	1110	1190	1190
$\rho(\text{CH}_2)(\text{B}_1)$	1250	990			840			620
			1215	1195–1240		1015	1025	
$\omega(\text{CH}_2)(\text{B}_2)$	1179	942			1160			865
lattice	161	152	170			160		

^a Also listed are the IR bands of solid H_2CO and D_2CO .

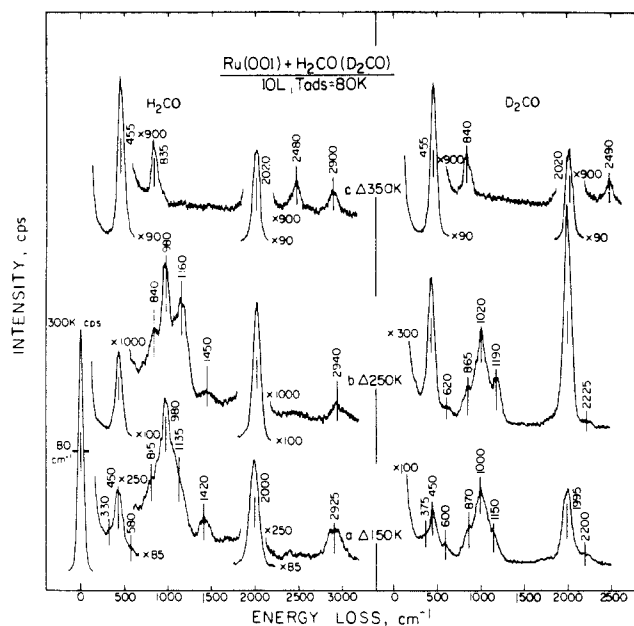


Figure 6. EEL spectra recorded after exposure of the clean Ru(001) surface to 10 L of H_2CO (left) and D_2CO (right) at 80 K. The symbol “ Δ ” signifies momentary heating of the surface to the indicated temperatures, followed by cooling to 80 K to record the spectra.

aldehyde from the clean surface between 120 and 160 K in the thermal desorption spectra of Figure 1. In the spectrum for H_2CO , Figure 6a's features which may be ascribed to vibrations or the frustrated translation of coadsorbed water are observed as shoulders on both the low and high frequency sides of the mode due to adsorbed CO at 450 cm^{-1} . A broad envelope of poorly resolved bands extends from 750 to 1250 cm^{-1} , a band due to C–H deformation vibrations is evident at 1420 cm^{-1} , and a band due to C–H stretching vibrations is evident at 2925 cm^{-1} . In the corresponding spectrum for D_2CO , a shoulder at 375 cm^{-1} on the low frequency side of the CO vibration at 450 cm^{-1} is observed, which again is due to the frustrated translation of D_2O perpendicular to the surface.⁴³ Also observed are a weak mode at 600 cm^{-1} , a broad, poorly resolved envelope of bands between 750 and 1250 cm^{-1} , and a weak feature due to C–D stretching modes at 2200 cm^{-1} . The increase in the intensity of $\nu(\text{CO})$ at 1995 – 2000 cm^{-1} in these spectra indicates that an additional 0.07–0.08 monolayer of formaldehyde decomposition has occurred upon annealing to 150 K.

The EEL spectra recorded after annealing to 250 K, Figure 6b, show no change in the intensities of the features due to adsorbed CO, indicating that decomposition has not occurred between 150 and 250 K. The remaining bands sharpen and decrease in intensity, consistent not only with some desorption of the adsorbed species which contribute to these bands but also with ordering of the remaining 0.03 monolayer of adsorbed species which has not decomposed. Results of other experiments for annealing temperatures between 250 and 300 K verify that the

features in Figure 6b at 840 , 980 , 1160 , 1450 , and 2940 cm^{-1} for H_2CO and at 620 , 865 , 1020 , 1190 , and 2225 cm^{-1} for D_2CO maintain their relative intensities and decrease in intensity in unison as the surface is annealed to progressively higher temperatures. As these vibrational features attenuate, those due to adsorbed CO increase in intensity. Consequently, these features are obviously due to a single adsorbed species which decomposes to yield CO in this temperature range.

Comparison of the frequencies observed in Figure 6b to those expected for paraformaldehyde [630 , 900 – 930 , 1090 – 1100 , 1235 , 1470 , and 2900 – 2980 for paraformaldehyde and 620 , 835 , 970 , 1050 – 1080 , 1130 – 1160 , and 2235 for paradideuterioformaldehyde⁵⁴] confirms that paraformaldehyde is not present on the surface. Similar comparisons allow species such as methoxy^{5,11} and η^2 -dioxymethylene,¹³ which have been observed as adsorbed products of the interaction of formaldehyde with other metal surfaces, to be excluded.

The spectra of Figure 6b are consistent with an η^2 configuration [see also Figure 5, bottom panel] for adsorbed formaldehyde, analogous to that obtained for the adsorption of acetone on the Ru(001) surface.²⁴ Assignments of each of the observed vibrational modes for both η^2 - H_2CO and η^2 - D_2CO are listed in Table II. The $\nu(\text{CO})$ frequency near 1000 cm^{-1} agrees well with those observed in analogous η^2 -formaldehyde complexes.^{18,19,21} In addition, the frequencies of the $\nu(\text{CH}_2)$, $\omega(\text{CH}_2)$, and $\rho(\text{CH}_2)$ modes agree well with assignments for methylene groups with sp^3 hybridization in other compounds, as do the frequency shifts upon deuteration [$(\nu$ for $\text{H}_2\text{CO})/(\nu$ for $\text{D}_2\text{CO}) = 1.32$ to 1.35].^{51,52,55} Noteworthy, however, is the slight increase from 980 to 1020 cm^{-1} of $\nu(\text{CO})$ upon deuteration and the less-than-expected⁵⁶ decrease from 1450 to 1190 cm^{-1} of $\delta(\text{CH}_2)$ upon deuteration [$\delta(\text{CH}_2)/\delta(\text{CD}_2) = 1.22$]. The origin of these effects can be explained in terms of a strong interaction between the $\nu(\text{CO})$ and $\delta(\text{CD}_2)$ modes of η^2 - D_2CO . The description of molecular vibrational motion in terms of bending and stretching of isolated units [e.g., $\delta(\text{CH}_2)$, $\nu(\text{CO})$, $\omega(\text{CH}_2)$, etc.] fails when two (or more) vibrational modes involving motion of common atoms and belonging to the same symmetry type have nearly equal frequencies.^{52,57} In this circumstance, the resulting normal modes of the molecule are combinations of the two (or more) types of motion, which may produce frequencies substantially different than are expected for vibrations of the isolated units. For η^2 - H_2CO , the $\nu(\text{CO})$ mode at 980 cm^{-1} and the $\delta(\text{CH}_2)$ mode at 1450 cm^{-1} , both of which are of A' symmetry for η^2 -formaldehyde in the expected C_s configuration and derived from A_1 modes of free formaldehyde (see Table II), are largely decoupled due to their disparity in frequency. Thus,

(54) Tadokoro, H.; Kobayashi, M.; Kawaguchi, Y.; Kobayashi, A.; Murahashi, S. *J. Chem. Phys.* **1963**, *38*, 703.

(55) Ibach, H.; Mills, D. L. “Electron Energy Loss Spectroscopy and Surface Vibrations”; Academic Press: New York, 1982.

(56) If hydrogen motion is decoupled from other vibrational motion of a molecule, substitution of deuterium for hydrogen decreases the frequencies of hydrogenic modes by the square root of the H/D mass ratio, and $\nu(\text{H})/\nu(\text{D}) = 1.41$.^{52,53}

(57) Colthup, N. B.; Daly, L. H.; Wiberley, S. E. “Introduction to Infrared and Raman Spectroscopy”; Academic Press: New York, 1975.

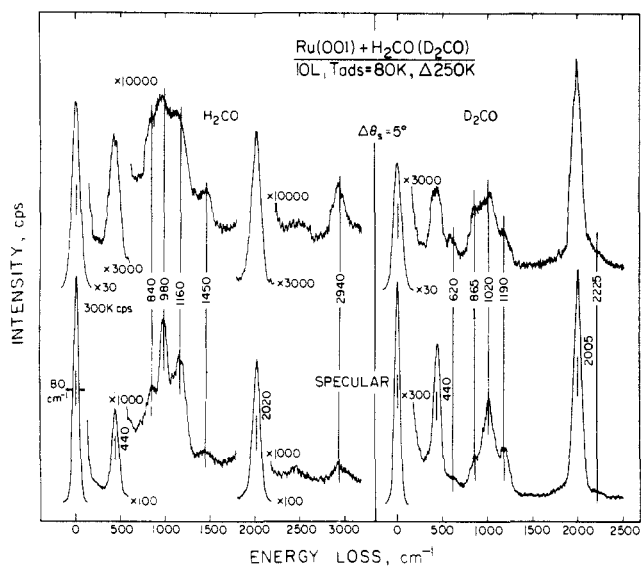


Figure 7. EEL spectra of η^2 -H₂CO (left) and η^2 -D₂CO (right) recorded in the specular direction (bottom) and 5° out of the specular direction (top).

the δ (CH₂) vibration involves almost exclusively relative motion of the hydrogen atoms, and the ν (CO) vibration involves only relative motion of the carbon and oxygen atoms. When deuterium is substituted for hydrogen, however, the frequency of isolated δ (CD₂) motion shifts to approximately $1450/1.41 = 1030$ cm⁻¹, where coupling with the ν (CO) motion is strong. Thus, the resulting normal mode for η^2 -D₂CO identified as δ (CD₂) actually involves substantial ν (CO) motion, and the mode identified as ν (CO) contains substantial δ (CD₂) motion.

In dipolar inelastic scattering, the electrons of the EELS beam incident upon the surface interact with the time-dependent electric field above the surface which results from the oscillation of separated charges in the adsorbed species, exiting the surface in the near specular direction after losing energy to excite a surface vibration.⁵⁵ Since the charge separation between the carbon and hydrogen (or deuterium) atoms of the C-H (or C-D) bonds is small with respect to that between carbon and oxygen of the C-O bond, strong dipolar scattering is only expected to occur for those vibrational modes of adsorbed formaldehyde which involve motion of the carbon and oxygen atoms with respect to each other. Since the cross section for dipolar inelastic scattering is strongly peaked in the specular direction, rotation of the electron energy analyzer away from the specular collection geometry where dipolar scattering is dominant attenuates features due to dipolar scattering, i.e., those vibrations which involve C-O motion for adsorbed formaldehyde, with respect to features due primarily to short-range impact scattering, i.e., those vibrations which involve mainly C-H (or C-D) motion for adsorbed formaldehyde.⁵⁵ This is clearly illustrated in Figure 7 for both η^2 -H₂CO and η^2 -D₂CO. Comparison of the top spectrum for η^2 -H₂CO, at the left of Figure 7, that was recorded with the electron energy analyzer rotated 5° in the scattering plane away from the specular direction toward the surface normal, to that below it for specular scattering shows that the ν (CO) mode at 980 cm⁻¹ is attenuated sharply with respect to the ρ -, ω -, δ -, and ν (CH₂) modes of η^2 -H₂CO at 840, 1165, 1450, and 2940 cm⁻¹, which maintain their relative intensities. In the spectra at the right for η^2 -D₂CO, however, both ν (CO) at 1020 cm⁻¹ and δ (CD₂) at 1190 cm⁻¹ are attenuated in unison upon changing from the specular to the off-specular scattering geometry, maintaining their intensities relative to each other but decreasing uniformly with respect to the ρ -, ω -, and ν (CD₂) modes at 620, 865, and 2225 cm⁻¹. The δ (CD₂) mode of η^2 -D₂CO at 1190 cm⁻¹ shows much stronger dipolar scattering than the corresponding δ (CH₂) mode of η^2 -H₂CO at 1450 cm⁻¹, illustrating the strong coupling of C-O and C-D motion in this vibrational mode of η^2 -D₂CO.

Returning to the spectra of Figure 6, the most notable effect of annealing to 350 K [Figure 6c] the Ru(001) surface, upon

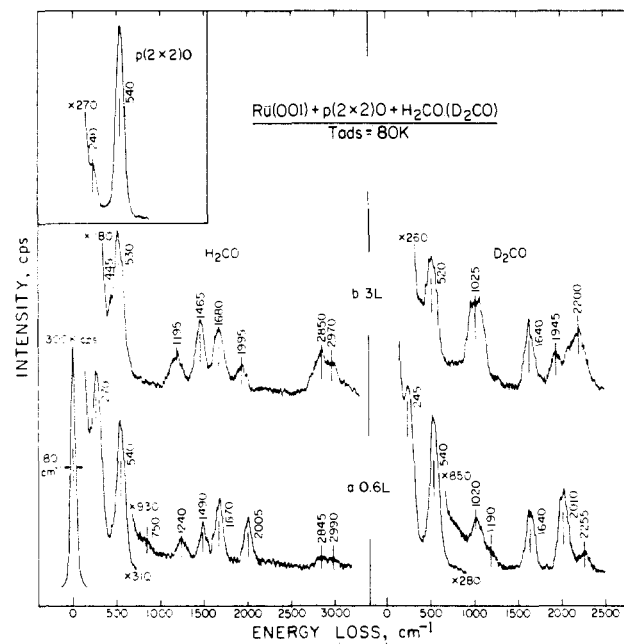


Figure 8. EEL spectra recorded after the indicated exposures of the Ru(001)-p(2 \times 2)O surface to H₂CO (left) and D₂CO (right) at 80 K. Also shown in the inset is the EEL spectrum of the p(2 \times 2) oxygen overlayer.

which η^2 -formaldehyde and CO and hydrogen from the decomposition of formaldehyde are adsorbed, is to decompose completely the remaining 0.03 monolayer of η^2 -formaldehyde. The CO coverage in spectra (c) of Figure 6 is approximately 0.25 monolayer, and, for coverages of CO above approximately 0.20 monolayer, the vibrational spectrum of adsorbed CO on Ru(001) not only shows modes at 455 and 2020 cm⁻¹ due to ν (RuC) and ν (CO), respectively, but also shows weak features at 2450–2490 cm⁻¹ due to the combination loss of ν (RuC) + ν (CO) and at 835–840 cm⁻¹ due to the overtone of ν (RuC), downshifted from twice the ν (RuC) frequency due to the anharmonicity of the ruthenium-carbon bond.³⁹ In addition to these features from adsorbed CO, the spectrum for H₂CO shows a weak feature at 2900 cm⁻¹ due to a small amount of an unidentifiable hydrocarbon fragment on the surface. Some spectra for both H₂CO and D₂CO recorded after annealing to temperatures between 250 and 350 K showed bands clearly attributable to small amounts (less than 0.01 monolayer) of coadsorbed η^2 -formate.⁵⁸ These bands are almost certainly due to small concentrations of impurities in the adsorbed formaldehyde and are insignificant.

D. EELS of Formaldehyde on the Ru(001)-p(2 \times 2)O Surface.

The EEL spectrum of the p(2 \times 2)O overlayer is shown in the inset of Figure 8. In addition to the feature at 540 cm⁻¹ due to motion of the oxygen adatoms in threefold hollow sites perpendicular to the surface, a mode appears at 240 cm⁻¹ which results from coupling of the overlayer to a ruthenium surface phonon.⁴⁰ The presence of the p(2 \times 2)O overlayer, with an ideal fractional surface coverage of 0.25, changes the work function of the Ru(001) surface by +0.20 eV.⁴¹ Employing a Ru=O bond length of 2.05 Å⁴⁰ and ignoring depolarization effects, this change in the work function is equivalent to the transfer of 0.02 electron from the ruthenium surface to each oxygen adatom of the p(2 \times 2)O overlayer,⁵⁹ producing a quantifiable increase in the Lewis acidity of the surface ruthenium atoms.

Spectra recorded after adsorption of 0.6 L of H₂CO and D₂CO on the Ru(001)-p(2 \times 2)O surface at 80 K are shown in Figure 8a. The strong mode due to adsorbed oxygen of the p(2 \times 2) overlayer is visible at 540 cm⁻¹, and a broad, weak feature due to librational modes of a small amount of coadsorbed H₂O can

(58) Avery, N. R.; Toby, B. H.; Anton, A. B.; Weinberg, W. H. *Surf. Sci.* **1982**, *122*, L574.

(59) Topping, J. *Proc. R. Soc. London, A* **1927**, *114*, 67.

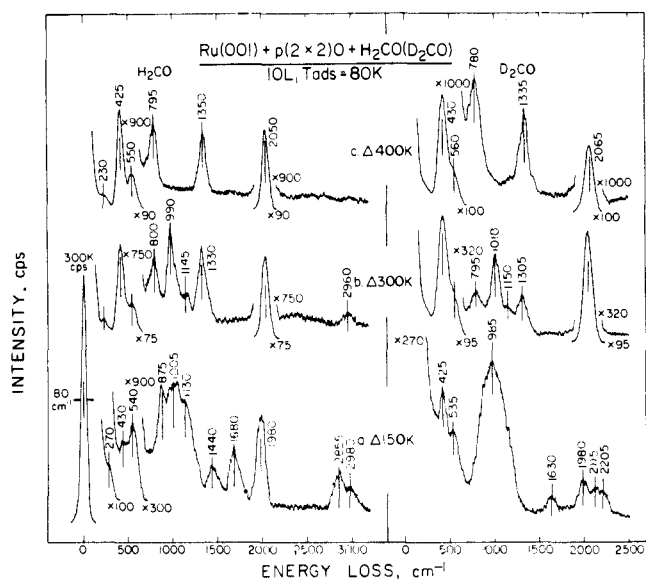


Figure 9. EEL spectra recorded after exposure of the Ru(001)-p(2×2)O surface to 10 L of H₂CO (left) and D₂CO (right) at 80 K, followed by annealing to the indicated temperatures.

be seen at 750 cm⁻¹ in the spectrum of H₂CO. Modes due to adsorbed CO from formaldehyde decomposition or background adsorption of CO are present in both spectra with intensities indicative of coverages near 0.01 monolayer. The remaining features in both spectra are due to the presence of η¹-formaldehyde. The band locations and assignments for η¹-H₂CO and η¹-D₂CO are listed in Table II. The strong band at 270 cm⁻¹ in the spectrum of H₂CO and the band at 245 cm⁻¹ in the spectrum of D₂CO are due to the frustrated translation of the η¹-formaldehyde perpendicular to the surface.

Spectra for 3-L exposures of H₂CO and D₂CO under the same conditions are shown in Figure 8b. Although there are slight changes in the frequencies and relative intensities of some modes, no clear evidence for any species on the Ru(001)-p(2×2)O surface other than η¹-formaldehyde and carbon monoxide is present in the spectra of Figure 8. This conclusion is in agreement with the results of a previous investigation of acetone adsorption on the clean Ru(001) and the Ru(001)-p(2×2)O surfaces,²⁴ where preadsorption of oxygen stabilized the η¹ form of adsorbed acetone with respect to the η² form.

Figure 9 shows spectra recorded after exposure of the Ru(001)-p(2×2)O surface to 10 L of H₂CO and D₂CO, an exposure that is more than sufficient to provide a saturated monolayer of formaldehyde at 80 K, followed by annealing to the indicated temperatures. The decrease in the intensities of the modes due to η¹-formaldehyde in the spectra of Figure 9a, measured after annealing to 150 K, compared to the spectra of Figure 8b, indicates that approximately 80% of the η¹-formaldehyde has desorbed by this temperature. This correlates with the thermal desorption peaks at 130 and 150 K for formaldehyde on the Ru(001)-p(2×2)O surface, shown in Figure 1. The attenuation of the bands due to η¹-formaldehyde is accompanied by the appearance of bands in the frequency range expected for η²-formaldehyde, at 875, 1005, 1130, and 1440 cm⁻¹ in the spectrum for H₂CO and a single, broad band centered at 985 cm⁻¹ in the spectrum for D₂CO.

Spectra recorded following annealing to temperatures between 150 and 300 K demonstrate that the broad envelope of bands between 750 and 1250 cm⁻¹ in the spectra for both H₂CO and D₂CO changes shape as a surface reaction proceeds which forms the products evident in the spectra of Figure 9b. Significant decomposition of η²-formaldehyde occurs in this temperature range, as evidenced by the increase in the intensities of the modes due to adsorbed CO. Furthermore, the bands due to η¹-formaldehyde decrease in intensity in this temperature range, and bands near 800 and 1300 cm⁻¹ grow concomitantly with the disappearance of the η¹-formaldehyde at annealing temperatures between 200 and 250 K. These bands are due to η²-formate⁵⁸

produced by the reaction of η¹-formaldehyde with the oxygen adatoms of the p(2×2)O overlayer. Slight desorption of η¹-formaldehyde also occurs in this temperature range, producing the very weak desorption rate maxima between approximately 180 and 300 K in the thermal desorption spectra of Figure 1 (right). No η¹-formaldehyde is evident in the EEL spectra for annealing temperatures greater than 250 K. At 300 K [Figure 9b], bands due to 0.04 monolayer of η²-formate are present at 800 and 1330 cm⁻¹ for H₂CO and at 795 and 1305 cm⁻¹ for D₂CO. In addition, bands due to 0.01 monolayer of η²-formaldehyde are evident at 990, 1145, and 2960 cm⁻¹ for H₂CO and at 1010 and 1150 cm⁻¹ for D₂CO. The high intensity of the ν(CO) mode in these spectra (990 and 1010 cm⁻¹) relative to the other modes of η²-formaldehyde is probably a result of the perturbation of its bonding interaction with the surface due to the presence of the coadsorbed oxygen of the p(2×2)O overlayer. This perturbation is also evidenced in the increased stability of η²-formaldehyde on the Ru(001)-p(2×2)O surface; on the clean Ru(001) surface, decomposition of η²-formaldehyde is complete by 300 K.

Annealing to 400 K decomposes the remaining η²-formaldehyde, decomposes a fraction of the η²-formate, and desorbs a fraction of the CO from the surface. The remaining η²-formate persists to 450 K on the Ru(001)-p(2×2)O surface, and its decomposition produces the broad, weak desorption feature for hydrogen between 400 and 470 K in Figure 3c.⁶⁰

EEL spectra recorded after annealing to temperatures sufficient to desorb all the hydrogen and CO from the surface show the features at 240 and 540 cm⁻¹ due to the p(2×2)O overlayer with intensities unchanged from those observed prior to the adsorption of formaldehyde at 80 K. This verifies that little or no consumption of the oxygen adatoms of the p(2×2) overlayer by reaction with formaldehyde or its dissociation products occurs under these experimental conditions.

IV. Discussion

The η¹ and η² coordination geometries identified for formaldehyde in the EELS results reported here can be understood qualitatively in terms of the interaction of the valence orbitals of the surface metal atoms with the highest occupied and lowest unoccupied molecular orbitals of free formaldehyde.²⁴ An η¹ coordination geometry results from overlap of a single lobe of the nonbonding oxygen lone pair orbital of formaldehyde [at 12.0 eV below the vacuum level for free formaldehyde⁶¹] with a ds hybrid acceptor orbital of the metal, resulting in a net transfer of electron density from the ligand to the metal surface. Presumably due to the low amplitude on the oxygen atom of the π_{CO}* antibonding orbital of formaldehyde [at 3.1 eV above the vacuum level⁶¹], little backdonation from the metal to this orbital occurs, as judged by the weak perturbation of the vibrational frequencies for η¹-formaldehyde relative to the frequencies of free formaldehyde (cf. Table II). The role of the metal in this type of interaction is that of a weak Lewis acid, and the resulting metal-formaldehyde bond is correspondingly weak. For example, the thermal desorption spectra of Figure 1 indicate binding energies between 7 and 9 kcal/mol⁴⁷ for the desorption features attributable to η¹-formaldehyde at 130 and 155 K.

An η² coordination geometry results from overlap of the π_{CO} bonding orbital of formaldehyde [at 14.6 eV below the vacuum level⁶¹] with a ds hybrid acceptor level of the metal, along with backdonation from the metal into the π_{CO}* antibonding orbital of the formaldehyde.⁶² The strength of this interaction, and, therefore, the probability of its occurrence relative to the η¹ interaction, depends critically on the ability of the ligand-metal bond to facilitate backdonation, since in the absence of backdonation the π donor bond is weaker than the lone pair donor bond which produces η¹ coordination. The importance of backdonation and

(60) Toby, B. H.; Avery, N. R.; Anton, A. B.; Weinberg, W. H., in preparation.

(61) Hess, B.; Bruna, P. J.; Bunker, R. J.; Peyerimhoff, S. D. *Chem. Phys.* **1980**, *18*, 267.

(62) Dewar, M. J. S. *Bull. Soc. Chim. Fr.* **1951**, *18*, C79. Chatt, J.; Duncanson, L. A. *J. Chem. Soc.* **1953**, 2939.

the function of the metal as a Lewis base in this type of interaction is evidenced in the results obtained in structural studies of η^2 -aldehyde complexes,^{18–22} where in all cases nearly complete rehybridization of the acyl carbon from sp^2 to sp^3 occurs, and the carbon–oxygen bond order for the aldehyde ligands is lowered to nearly one.

The π_{CO}^* antibonding orbital of free formaldehyde is approximately 1.3 eV lower in energy than the corresponding orbital of free acetone [π_{CO}^* at 4.4 eV above the vacuum level for acetone⁶¹]. This decreases the disparity in energy between this orbital for formaldehyde and the highest occupied levels of the metal with which it interacts in η^2 bonding, facilitating increased backdonation for formaldehyde with respect to acetone. Several aspects of the comparative chemistry of these two ligands can be correlated with this difference. First, the only η^2 -acetone complex isolated thus far has the acetone coordinated to an electropositive tantalum center,⁶³ whereas η^2 -formaldehyde complexes have been synthesized with more electronegative osmium¹⁸ and ruthenium²⁰ centers. Furthermore, η^2 -formaldehyde on Ru(001) shows $\nu(CO)$ near 1000 cm^{-1} , whereas $\nu(CO)$ for η^2 -acetone on Ru(001) is near 1300 cm^{-1} ,²⁴ indicating more extensive rehybridization of the acyl carbon due to backdonation for η^2 -formaldehyde than for η^2 -acetone. Finally, the more extensive rehybridization evident for η^2 -formaldehyde on Ru(001) results in a lower barrier to its dissociation, explaining the fact that significant decomposition of formaldehyde, presumably through η^2 -formaldehyde and η^2 -formyl intermediates, occurs on the clean Ru(001) surface at 80 K (cf. Figure 4), whereas decomposition of η^2 -acetone on the same surface begins near 200 K.²⁴

It is interesting to compare data for the η^2 -formaldehyde ligand in organometallic complexes with our results for η^2 -formaldehyde on Ru(001). The interaction of formaldehyde with single osmium¹⁸ and vanadium¹⁹ centers as well as the oxidation of coordinated methylene at a rhenium center²⁰ produces the η^2 -formaldehyde configuration shown in (b) in the bottom panel of Figure 5 (R = H). The carbonylation of a zirconium hydride forms a bridging η^2 -formaldehyde,²¹ as in (c) in the bottom panel of Figure 5. Also of interest is a configuration like that of (d), which has been observed for η^2 -acetaldehyde (R = CH_3) in a dimolybdenum complex.²² All of these compounds have carbon–oxygen bond lengths between 1.35 and 1.59 Å, and those that have been characterized by vibrational spectroscopy have $\nu(CO)$ between 1012 and 1160 cm^{-1} , in good agreement with our results for η^2 -formaldehyde on Ru(001). The low frequency of $\nu(CO)$ for η^2 -formaldehyde both on the Ru(001) surface and in these organometallic compounds clearly indicates that the acyl carbon has undergone extensive rehybridization from sp^2 to sp^3 . A distinction among these possible bonding configurations for η^2 -formaldehyde on Ru(001) is not possible, since the vibrational spectra would differ only in the unresolved, low frequency vibrations which involve motion of the bonds that coordinate the η^2 -formaldehyde to the surface.

Although little vibrational data exist for η^2 -formyl ligands in homogeneous organometallic compounds, several structures of η^2 -formyl have been characterized analogous to those shown in (b),³⁰ (c),³¹ and (d)³² in the top panel of Figure 5. Those with the structure (b), in which the carbon and oxygen atoms are coordinated to a single metal atom, show $\nu(CO)$ frequencies between 1450 and 1600 cm^{-1} , and the low frequency (1180 cm^{-1}) for $\nu(CO)$ of η^2 -formyl on Ru(001) thus suggests that the η^2 -formyl on this surface is coordinated to at least two surface ruthenium atoms. Hence, structures (c) and (d) are regarded as the most likely for η^2 -formyl on Ru(001).

It should be noted that a detailed analysis of the point-group symmetry properties of the adsorbate complex, as was carried out successfully for η^1 - and η^2 -acetone on Ru(001),²⁴ cannot be done in a straightforward manner for adsorbed formyl or the adsorbed formaldehyde species on Ru(001). Since the dominant contribution to inelastic electron scattering from hydrogenic vibrations is expected to be via an impact rather than a dipolar mechanism

at the electron beam energy employed for the EELS measurements reported here, all vibrations involving hydrogenic motion are, in principle, active in both specular and off-specular EELS measurements.⁵⁵ For a molecule like formaldehyde in which the skeletal configuration is defined by the orientations of C–H bonds, the polarizations of skeletal vibrations with respect to the symmetry elements of the adsorbate–surface complex cannot be determined by the standard technique of noting the dipolar activity (or inactivity) of signature skeletal modes for specular scattering and applying the “dipolar selection rule”⁵⁶ to determine bond orientations. For example, the appearance of the $\pi(CH)$ vibration in the spectra for η^2 -formyl does not rule out the possibility that the η^2 -formyl is adsorbed in a configuration with C_s symmetry (with the carbon, hydrogen, and oxygen atoms lying in a mirror symmetry plane perpendicular to the surface), even though the $\pi(CH)$ mode would be dipolar inactive in this configuration. Indeed, C_s symmetry is expected for both η^2 -formaldehyde and η^2 -formyl on Ru(001), in analogy to η^2 -acetone.

The conditions that lead to the formation of η^2 -formyl and η^2 -formaldehyde provide a consistent picture of the mechanism of formaldehyde decomposition on the clean Ru(001) surface. For low exposures of formaldehyde to Ru(001) at 80 K, total decomposition to adsorbed CO and hydrogen occurs. This indicates that the activation energy for dissociation of η^2 -formaldehyde on Ru(001) at low coverages is less than 4.8 kcal·mol⁻¹.⁶⁴ As binding sites for the hydrogen from decomposition are occupied, further decomposition is inhibited sterically, stabilizing both the partial decomposition product η^2 -formyl over a small exposure range [Figure 4a] and η^1 - and η^2 -formaldehyde at coverages approaching a saturated monolayer [Figure 4b]. Annealing to temperatures below the onset of hydrogen desorption renders probable the complete decomposition of η^2 -formyl and additional decomposition of η^2 -formaldehyde, as η^1 -formaldehyde is desorbed and hydrogen adatoms become mobile, exposing the necessary binding sites for the products of η^2 -formaldehyde decomposition. For example, the *apparent* activation energy for the decomposition of η^2 -formaldehyde at 150 K, 9 kcal·mol⁻¹, represents the steric barrier which η^2 -formaldehyde must overcome under these conditions to find binding sites to accommodate the decomposition products, hydrogen and CO, on the surface. These conclusions are supported by the results of EELS measurements for adsorption of formaldehyde at 80 K on the Ru(001) surface precovered with a saturated monolayer of hydrogen adatoms.⁴⁸ Only η^1 - and η^2 -formaldehyde are observed at 80 K for all submonolayer coverages, and very little decomposition is observed until hydrogen desorption commences near 275 K, whereupon decomposition of η^2 -formaldehyde proceeds rapidly.

The effect of hydrogen coverage on the rate of dissociation of η^2 -formaldehyde has another important consequence for the interpretation of the experimental results reported here. If η^2 -formaldehyde has a characteristic activation energy for *molecular desorption* (i.e., heat of adsorption) less than the activation energy for recombination and desorption of hydrogen from the Ru(001) surface, at high surface coverages, where the binding sites for the products of the decomposition of η^2 -formaldehyde on the Ru(001) surface are filled and further decomposition is unfavorable, molecular desorption of η^2 -formaldehyde would occur. Consequently, the desorption of molecular formaldehyde from the clean surface at 275 K for high surface coverages (cf. Figure 1) is due to the desorption of η^2 -formaldehyde. The high binding energy of this adsorbed species on Ru(001) (approximately 115 kcal·mol⁻¹) makes the formation of η^2 -formaldehyde far more favorable than the formation of paraformaldehyde on the Ru(001) surface. This estimate of the binding energy is based on the observed rehybridization of the η^2 -formaldehyde and should not be confused with the activation energy of desorption of η^2 -formaldehyde which

(64) The activation energies for these surface reactions are estimated by assuming first-order kinetics, which is appropriate for unimolecular decomposition reactions, and assuming a preexponential factor of the reaction rate coefficient of 10¹³ s⁻¹. The activation energy, E_a , is then obtained by assuming that the characteristic time of the reaction is approximately 1 s, i.e., 10⁻¹³ exp(E_a/kT).

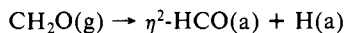
(63) Wood, C. D.; Schrock, R. R. *J. Am. Chem. Soc.* **1979**, *101*, 5421.

is approximately 16 kcal·mol⁻¹.

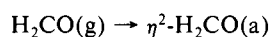
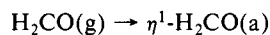
The results of these considerations for the surface chemistry of formaldehyde adsorbed on both the clean and Ru(001)-p-(2×2)O surfaces may be illustrated by overall reaction schemes for the monolayer species adsorbed on both surfaces. Initial exposure of the clean Ru(001) surface to formaldehyde at 80 K produces adsorbed CO and hydrogen from decomposition



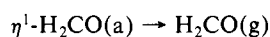
Once decomposition has progressed to approximately 0.15 monolayer of formaldehyde, subsequent exposure produces 0.02–0.03 monolayer of η^2 -formyl



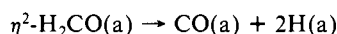
Heating the surface upon which η^2 -formyl is adsorbed to 120 K decomposes the η^2 -formyl. Further exposure to formaldehyde produces both η^1 -formaldehyde and 0.10 monolayer of η^2 -formaldehyde



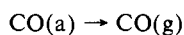
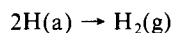
The η^1 -formaldehyde desorbs molecularly between 120 and 160 K



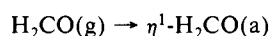
exposing binding sites for the products of the decomposition of 0.07–0.08 monolayer of η^2 -formaldehyde



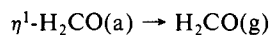
As the surface is heated to 300 K, hydrogen desorption begins, and decomposition of the remaining 0.03 monolayer of η^2 -formaldehyde follows rapidly. Hydrogen is evolved from the surface in a desorption rate-limited step between 250 and 350 K, and CO is evolved from the surface in a desorption rate-limited step at 480 K



Exposure of the Ru(001)-p-(2×2)O surface to formaldehyde at 80 K produces η^1 -formaldehyde



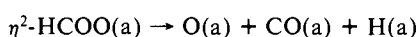
Negligible decomposition of formaldehyde is observed under these conditions. Heating the surface to 150 K desorbs approximately 80% of the η^1 -formaldehyde



with conversion also to η^2 -formaldehyde. Further heating of the surface to 300 K produces approximately 0.08 monolayer of CO from the decomposition of η^2 -formaldehyde and produces approximately 0.04 monolayer of η^2 -formate from the reaction of η^1 -formaldehyde with the oxygen adatoms of the p(2×2)O overlayer

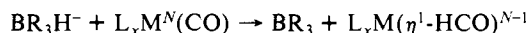


This reaction as well as the decomposition of η^2 -formaldehyde produces hydrogen above its characteristic temperature of desorption from the Ru(001)-p-(2×2)O surface. Thus hydrogen atom recombination and desorption follow rapidly in the temperature range between 250 and 300 K. Approximately 0.01 monolayer of η^2 -formaldehyde remains on the surface at 300 K. Further heating decomposes the remaining η^2 -formaldehyde, and decomposition of the η^2 -formate occurs between 400 and 450 K



Again, hydrogen desorption follows rapidly. The CO from decomposition is evolved from the surface in a desorption rate-limited step at 450 K. The p(2×2) oxygen overlayer is left intact on the surface.

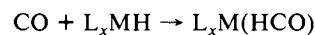
The appearance of η^2 -formyl as an intermediate to the decomposition of adsorbed formaldehyde on Ru(001) has important implications for the mechanistic understanding of surface catalyzed CO hydrogenation reactions.^{15,65} Although the reaction of coordinated CO with hydrogen from borohydride donors has been shown to produce η^1 -formyl complexes of rhenium^{26,27} and iron²⁹ under homogeneous conditions, this reaction, represented schematically as [R = alkyl or alkoxide, L = Cp, PPh₃, NO, CO, and/or P(OC₆H₅)₃]



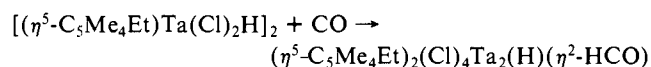
involves direct nucleophilic attack by the electron-rich hydrogen atom of the hydride donor at the carbonyl carbon. The resulting compounds are either neutral [$N = +1$]^{26,27} or are negatively charged [$N = 0$]. At no point is molecular hydrogen, nor an intermediate *metal* hydride, involved in this elementary reaction. Furthermore, the resulting η^1 -formyl is only weakly stable, and the weakened carbon–oxygen bond of η^1 -formyl relative to that of the CO which can be formed by its decomposition to the hydrido-carbonyl product drives the equilibrium for the decomposition reaction, represented below, to the right^{15,27,30,32}



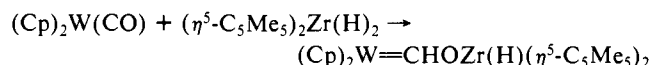
A more realistic model of the elementary CO reduction reaction which must occur under heterogeneous catalytic conditions involves migratory insertion of CO into a metal hydride bond⁶⁵



Thus far, only one such reaction has been observed under homogeneous conditions, where the reaction of CO with an oxophilic thorium hydride [$(\eta^5\text{-C}_5\text{Me}_5)_2\text{Th}(\text{H})(\text{OR})$, OR = alkoxide ligand³⁰] produces an η^2 -formyl like that shown in Figure 5b (upper panel). The ability of the single metal center to coordinate the formyl product in an η^2 configuration was considered crucial to the occurrence of this reaction, since the metal–oxygen bond which is formed increases the stability of the formyl product, shifting the equilibrium for the formyl decomposition reaction toward the desired η^2 -formyl product and away from the hydrido-carbonyl product.^{30,32,65} Another route to stabilization of the formyl product involves the use of multiple coordination centers for the CO hydrogenation reaction. Two such reactions have been observed under homogeneous conditions, one involving the reaction of CO with a tantalum hydride dimer³¹



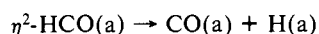
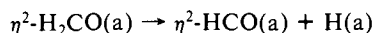
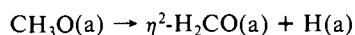
to produce an η^2 -formyl product, the structure of which is like that of Figure 5c (upper panel), and another involving the reaction of a tungsten carbonyl compound with a zirconium hydride³²



to produce a “carbene-like” η^2 -formyl complex, the structure of which is like that of Figure 5d (upper panel). The η^2 interaction not only stabilizes the η^2 -formyl intermediate, increasing the likelihood of its formation, but also increases the likelihood of subsequent attack by hydrogen to form formaldehyde intermediates, leading to oxygenated products, and to carbon–oxygen bond cleavage, leading to hydrocarbon products.⁶⁵

From these results concerning the mechanism of CO activation and reduction under homogeneous conditions, the importance of the η^2 -formyl observed in the decomposition of formaldehyde on Ru(001) is clearly evident. This result illustrates the ability of an extended metal surface to provide the proper coordination geometry for this species and supports strongly a surface reaction mechanism for CO hydrogenation which proceeds through an η^2 -formyl intermediate. This, coupled with the isolation of stable η^2 -formaldehyde on Ru(001), supports also the following reaction mechanism for methanol decomposition on Ru(001)⁵ and suggests

that the reverse reactions may well represent a plausible path for methanol synthesis on Ru(001):



It is interesting to note that a reaction sequence analogous to the reverse of the above set of reactions has been postulated to explain the formation of methanol from CO and hydrogen by $\text{Ru}_3(\text{CO})_{12}$ under homogeneous reaction conditions.¹⁷ Our observations should be interpreted as lending support to this proposition.

V. Summary

The important conclusions of this work may be summarized as follows: 1. Initial adsorption of formaldehyde on the clean Ru(001) surface at 80 K is dissociative, producing adsorbed CO and hydrogen. As binding sites for hydrogen adatoms become occupied, the total decomposition is inhibited, leading first to the formation of η^2 -formyl and then to molecular adsorption of formaldehyde in both η^1 and η^2 configurations. 2. Heating of the clean surface after a monolayer saturation exposure to formaldehyde at 80 K causes the η^1 -formaldehyde to desorb molecularly and the η^2 -formaldehyde to decompose (to adsorbed CO and

hydrogen). The clean Ru(001) surface is active for the decomposition of approximately a quarter-monolayer of formaldehyde under these conditions. 3. The presence of a $p(2 \times 2)$ oxygen overlayer on the Ru(001) surface increases the Lewis acidity of the surface ruthenium atoms, and adsorption of formaldehyde at 80 K on the Ru(001)- $p(2 \times 2)$ O surface produces vibrational spectra characteristic of η^1 -formaldehyde for all submonolayer coverages. 4. Heating of the Ru(001)- $p(2 \times 2)$ O surface after a monolayer saturation exposure to formaldehyde at 80 K causes the η^1 -formaldehyde to desorb molecularly, with some conversion to η^2 -formaldehyde. In addition to decomposition of the η^2 -formaldehyde to CO and hydrogen, reaction of η^1 -formaldehyde with the oxygen adatoms of the $p(2 \times 2)$ O overlayer to produce η^2 -formate occurs between 150 and 300 K. The Ru(001)- $p(2 \times 2)$ O surface is active for approximately one-half as much formaldehyde decomposition (via both η^2 -formaldehyde and η^2 -formate intermediates) as the clean surface under these conditions. 5. The appearance of η^2 -formyl and η^2 -formaldehyde as stable intermediates in the decomposition of formaldehyde on Ru(001) supports a reaction mechanism for CO hydrogenation to methanol under heterogeneous conditions which includes these species as important intermediates.

Acknowledgment. This research was supported by the National Science Foundation under Grant No. CHE-8516615.

Registry No. HCHO, 50-00-0; CO, 630-08-0; Ru, 7440-18-8.

Substrate Effect on Flavin-Enzyme Interaction in *p*-Hydroxybenzoate Hydroxylase as Probed by Resonance Inverse Raman Spectroscopy

Rachelle J. Bienstock,[†] Lawrence M. Schopfer,[‡] and Michael D. Morris*[†]

Contribution from the Departments of Chemistry and Biological Chemistry, University of Michigan, Ann Arbor, Michigan 48109. Received June 17, 1985

Abstract: Binding between the FAD and apoprotein of *p*-hydroxybenzoate hydroxylase (E.C. 1.14.13.2) from *Pseudomonas fluorescens* has been examined by using resonance inverse Raman spectroscopy. The vibrations of the flavin chromophore have been studied in the presence of substrates (*p*-hydroxybenzoate, 2,4-dihydroxybenzoate, and *p*-aminobenzoate), inhibitors (chloride and azide), and an effector (6-hydroxynicotinate). Ternary systems involving enzyme, inhibitor, and substrate were also examined. The 1195- and 1418-cm⁻¹ bands are significantly shifted in frequency upon binding either substrate, inhibitor, or effector. The 1163-, 1311-, and 1595-cm⁻¹ bands shifted in the presence of inhibitor, effector, or in the ternary complex, but not in the presence of substrate, alone. The 1184-cm⁻¹ band was affected by azide and 6-hydroxynicotinate. The 1241-cm⁻¹ band was perturbed in the presence of 2,4-dihydroxybenzoate. Both the 1241- and 1258-cm⁻¹ bands were shifted in the ternary complexes and in the presence of 6-hydroxynicotinate. The 1284-cm⁻¹ band was shifted in azide. The intense 1355/1370-cm⁻¹ band was unchanged. The 1563-cm⁻¹ band in the free enzyme was unchanged by *p*-hydroxybenzoate, chloride, 6-hydroxynicotinate, and azide plus 2,4-dihydroxybenzoate but was shifted to higher wavenumbers in azide and did not appear in *p*-aminobenzoate, 2,4-dihydroxybenzoate, and azide plus *p*-hydroxybenzoate. These changes in flavin vibrational frequencies reflect conformational changes in the enzyme upon binding ligands. Hydrogen bonding between FAD at N(1), C(2)=O, N(3), C(4)=O, and amino acid chains 45-47 and 299-300 was strengthened by binding inhibitors, effectors, and substrates causing the shifts seen in the Raman spectra.

p-Hydroxybenzoate hydroxylase (E.C. 1.14.13.2) is an NADPH dependent flavoenzyme which hydroxylates *p*-hydroxybenzoic acid to form 3,4-dihydroxybenzoate.¹ The reaction is a two-step process in which molecular oxygen is consumed.¹⁻³ In the first step, the oxidized enzyme combines with *p*-hydroxybenzoate and NADPH, then the bound FAD is reduced by NADPH. In the second step, the reduced enzyme-substrate complex reacts with molecular

oxygen to yield a flavin-activated oxygen species. The substrate is hydroxylated, the oxidized FAD is regenerated. The complexes investigated in this work all involve oxidized enzyme and either substrate, effector, or inhibitor. They are made in the absence of the reducing agent NADPH and as such are intrinsically stable.

There have been many kinetic studies of the reactions catalyzed by this enzyme.¹⁻⁶ The crystal structure of the enzyme-*p*-

[†] Department of Chemistry.

[‡] Department of Biological Chemistry.

(1) Spector, T.; Massey, V. *J. Biol. Chem.* **1972**, *247*, 4679-4687.